

Nash Bargaining Optimization of Released Water from a Reservoir Dam under Climate Change Conditions (Case Study: Doiraj Dam)

Z. Pourkheirollah¹, M. Hafezparast Mavaddat^{1*}, and S. E. Fatemi¹

ABSTRACT

There is a growing demand for solving conflicts among water users and stakeholders under climate change conditions. This study applied ten CMIP5 climate models under the RCP8.5 scenario to simulate Doiraj Reservoir water allocation in Ilam Province. To reduce the uncertainty of climate models, the MOTP method was used by combining different GCM models. To predict reservoir inflow, the IHACRES Rainfall-Runoff model was considered and validated for the 2016 to 2044 time periods. Climate and hydrological indicators were extracted to monitor drought periods in the current and future projections. The WEAP model and the Asymmetric NASH Bargaining Method were used to simulate the water basin system and solve the conflict between stakeholders based on their utility functions, respectively. The results indicated that the rainfall would increase by 17.1 and 11.1% in spring and autumn and decrease by 9.4% in winter in the future projection. Furthermore, the highest temperature and runoff growth rate increased by 1.95°C in September and 6.3% compared to the base period, while demands would be increased by 55.75%. The long-term agricultural deficit are obtained as 10.9 and 10.2% by the WEAP model in the current and future conditions. Finally, the duration curve of reservoir storage showed that 20% of the time, the reservoir storage is empty for the Standard Operation Policy (SOP). By switching to the Nash bargaining policy, not only the minimum storage capacity reached 18 MCM for all the time, but also the effects of climate change would be adapted in the future, and the utility functions of all stakeholders would be satisfied as well.

Keywords: Climate models, CMIP5, Drought, IHACRES, Water resources management, WEAP model.

INTRODUCTION

Water resources management has become more complicated due to various parameters affecting water systems. For example, climate change, growing demands, changing of socio-economic conditions, environmental considerations, and hydrologic conditions have changed (Bozorg-Haddad *et al.*, 2018). The water supply of Dehloran Plain, the agricultural and industrial hub of Ilam Province, has increased temperatures in recent years. The Nash bargaining method and optimizing

allocation are necessary to resolve the conflict between those stakeholders in the border area. The standard form of water policy is replaced by conflict resolution methods with increasing conflicts between stakeholders in allocating water resources (Naghdi *et al.*, 2021).

Watershed stakeholders' conflict resolution for various environmental, agricultural, and industrial purposes is one of the most critical issues considered in water resources management. The use of the Game Theory approach to analyze water resource management problems has been

¹ Department of Water Engineering, Campus of Agriculture and Natural Resources, Razi University, Kermanshah, Islamic Republic of Iran.

* Corresponding author; e-mail: m.hafezparast@razi.ac.ir.



growing since 1942 (Ransmeier, 1942), and the Nash Bargaining Model is sixty-seven years old. However, they are not yet ready for retirement because they still produce effective ways to manage water allocation (Serrano, 2021). Water plays a vital role in every aspect of human life and has various geographical, social, and economic factors, making water resources an important source of conflict. Thus, decision-makers require reliable models with high precision to allocate water resources among different stakeholders (Leong and Lai, 2017). Multiple methods for conflict resolution exist, but non-cooperative resolution methods have gained attention from researchers because of their ability to prioritize influential stakeholders. Looking at the literature, an Asymmetric Nash Solution was developed to calculate the benefits of reducing groundwater pollution in a joint project between Mexico and the US (Frisvold and Caswell, 2000). Coppola (2000) resolved the conflict between various users of groundwater resources and prevented them from being contaminated. Additionally, Homayounfar *et al.* (2015) demonstrated that their suggested models could remarkably decrease the runtime and prevent dimensionality problems when comparing discrete dynamic game models. Fu *et al.* (2018) provided an asymmetric model for resolving conflicts of interest in trans boundary river water allocation problems for the Huaihe River Basin in China.

The climate changes affected the hydrological cycle and caused increased variability in water supplies across time and space and, consequently, uncertainty in water allocation decisions. Changes in precipitation and temperature and the effect of these parameters on runoff were investigated using CMIP5 models (Zheng *et al.*, 2018). In a study, Kaini *et al.* (2020) used 105 and 78 GCM models for RCP4.5, and 8.5 emission scenarios, respectively, and developed an envelope-based selection method for selecting representative GCMs

for the Kushi River Basin in China and Nepal.

Kalhari *et al.* (2022) examine the uncertainty of TAR and AR5 models on the impact of climate change on Khorram-Abad Basin runoff in Iran with the IHACRES model for the periods of 2040-2069 and 2070-2099. To investigate optimal water allocation of surface and groundwater resources under climate change, Moghadam *et al.* (2022) used the IHACRES runoff model to predict runoff for future climate conditions. Simulation results from IHACRES are the WEAP model's input to develop operational policies for the combined use of water resources. The average annual runoff under climate change conditions was simulated by IHACRES model in the period (1987-2000) and (2026-2039). The results show that it would decrease by about 1% in the future. They found out at what level of the reservoir the best water quality can be released. (Azadi *et al.*, 2019).

In the climate change condition, with increasing water demands, environmental flow could be supported by renewable energy. It is vital to the wide expansion of small-scale hydroelectric power plants, especially runoff-river power plants. (Kuriqi *et al.*, 2019; Malka *et al.*, 2022). The SSWI, SPI, and SRI indices are applied to investigate agricultural, meteorological and hydrological droughts, respectively, from 2020 to 2049 in China (Guoyong *et al.*, 2015). They used 5 models of the fifth IPCC report, and the results showed that the long-term agricultural droughts from 6 to 26 months occurred more than the other droughts.

The impact of climate change on water resources is analyzed by Mehrparvar *et al.* (2019). The conflict between IRWC and AJO stakeholders in the Zayandehrud Basin is modeled by the conflict resolution GMCR method and the WEAP model. Stakeholders often have different interests that can cause conflict and competition in common resources (Ratner *et al.*, 2018). Currently, conflict resolution models based on climate

change situations incorporate different decision-makers views into one system and gradually replace single or multi-criteria decision-making models (Sharifazari *et al.*, 2021).

In the SOP policy, the total shortage is minimized, but the severity of the shortages is high. This method encounters problems in times of drought. Therefore, the combination of the WEAP simulation model and game theory method in dry months significantly reduces the severity of failure in supplying the needs of the region during the operation period (Jeong and Kang, 2021).

To our knowledge, no research has been developed based on considering water resources simulation, climate change, and conflict resolution theory to monitor water allocation systems in drought regions. Additionally, in the previous studies, usually linking simulation and optimization platforms have been used, which has significantly ignored the effects of climate change. The main objective of the current research was to resolve disputes between industrial, agricultural, and environmental stakeholders in drought conditions. In this way, the GA and Nash Bargaining Method can optimize the allocation of surface and groundwater resources under climate change conditions.

MATERIALS AND METHODS

This study was conducted through four main stages: In the first stage, the climate parameters were assessed by 10 GCM models. In the second stage, the IHACRES hydrological model predicted the runoff, and the hydrological and climate indicators were calculated for the current and future projection. In the third stage, water system allocation was simulated by WEAP. In the fourth stage, water allocation to different stakeholders was optimized by the Asymmetric Nash bargaining method in the GA model. Figure 1 shows the flow chart of the methodology.

Case Study and the Problem Statement

Doiraj Reservoir is located in the southwest of Ilam Province, with total capacity of 191 MCM and 60 m in height. The most precipitation falls during December and January. Dehloran City, with more than 220 meters above sea level, is located at a low altitude in the western Zagros Mountains. The city generally has warm summers, while winters are relatively mild due to the low elevation, with an average annual rainfall of about 258 mm and is defined as an arid region. This area suffers from water conflicts among farmers of Dehloran and Musian agricultural plain, and 24 and 31 MCM for industrial and environmental water demands, as presented in Figure 2.

On the other hand, the border city of Dehloran, as an agricultural hub of the Ilam Province, is located in a sensitive area, and supplying water demands plays an important role in ensuring the security of this area.

Climate Scenarios and Uncertainty Analysis

The RCP scenarios and the future policies have predicted the climate condition by AR5 up to the year 2100 (IPCC, 2013). The details of 10 CMIP5 climate models are presented in Table 1.

Investigating the uncertainty of the output of each climate model requires uncertainty analysis calculations.

The main sources of uncertainty in climate change simulations at the regional scale are uncertainty in greenhouse gas emission scenarios, uncertainty in GCM simulations, and internal differences and uncertainties in several downscaling methods of GCM simulations (Giorgi and Francisco, 2001). In addition, in studies evaluating the impact of climate change, the forecasts do not have sufficient confidence due to the influence of various sources of uncertainty in the output of the forecasting system. Therefore, using the maximum number of available GCM

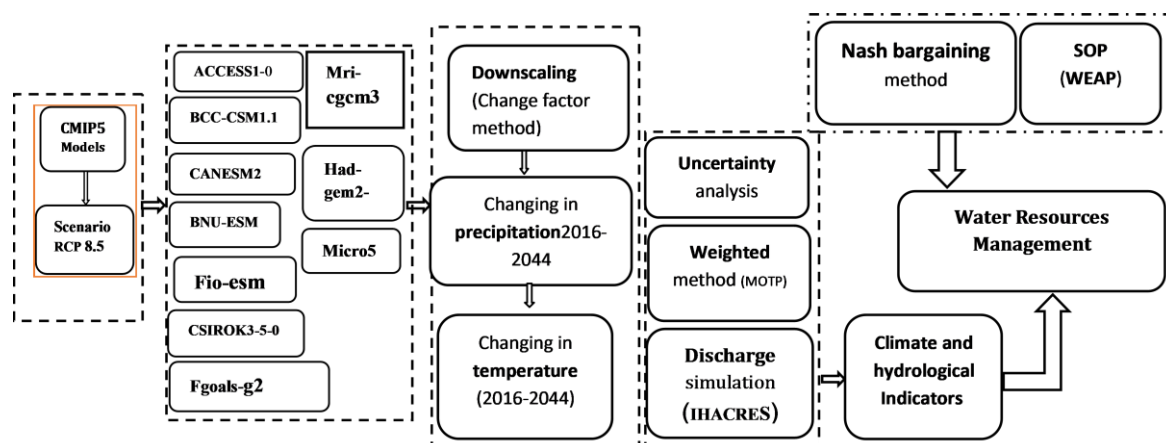


Figure 1. Flowchart of this research.

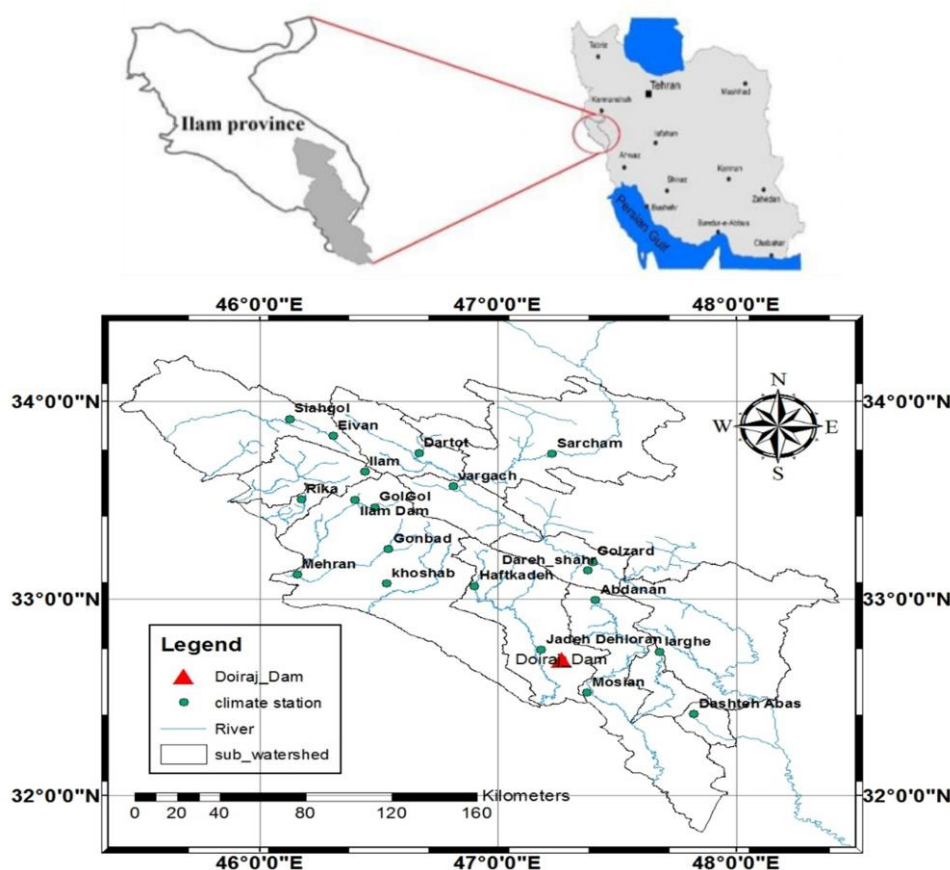


Figure 2. Location of the study area and climate stations in Ilam Province, Iran.

Table 1. CMIP5 models and their resolution.

Model name	CSIROK3-5-0	BNU-ESM	CANESM2	BCC-CSM1.1	ACCESS1-0	Fio-esm	Mri-cgcm3	Had-gem2-cc	Micro5	Fgoals-g2
Resolution	1.86×1.87	2.81×2.78	2.81×2.79	2.81×2.77	1.875×1.25	64×128	1.125×1.125	1.875×1.25	1.40×1.40	2.815×3.0

models in simulations is recommended to quantify the range of uncertainty in predictions (Jones 2000; Wilby and Harris 2006). Comparative studies between GCMs show that different models simulated meteorological variables with different degrees of accuracy and no single model provides the best simulation for all variables or regions (Lambert and Boer 2001). To assign the weighted mean of the variables in the GCMs' projections showed that these models incorporate a level of uncertainty for ensemble-based climate simulations (Christensen, 2010).

In this study, the MOTP method is utilized to determine the uncertainty of climate models. The first step is to collect monthly temperature and precipitation data for the period 1987 to 2015 and the future time 2016 to 2044.

The weighted GCMs are based on the deviation of its baseline simulated mean temperature and precipitation from its mean observation. In other words, GCMs, with greater weights, can predict climatic variables with more accuracy in the future (Mosadegh and Babaeian, 2022; Kalhori *et al.*, 2022).

$$W_i = \frac{(1/\Delta T_i)}{\sum_{i=1}^N (1/\Delta T_i)} \quad (1)$$

Where, W_i is the Weight of each model in the month i , N is the Number of total GCMs and ΔT_i is the difference between average of Temperature simulated by GCM $_j$ in the month i from the corresponding observed value.

$$\Delta T_i = \bar{T}_{AOGCM, Fut, i} - \bar{T}_{AOGCM, Base, i} \quad (2)$$

$$\Delta P_i = \left(\frac{\bar{P}_{AOGCM, Fut, i}}{\bar{P}_{AOGCM, Base, i}} \right) \quad (3)$$

$$T = T_{Obs} + \Delta T \quad (4)$$

$$P = P_{Obs} \times \Delta P \quad (5)$$

Where, ΔT_i and ΔP_i are climate change scenarios related to Temperature and Precipitation, respectively, for the month i ($1 \leq i \leq 12$); $\bar{T}_{AOGCM, fut, i}$ is the simulated future average Temperature of 28 years derived from each climate model for the month i ; and $\bar{T}_{AOGCM, base, i}$ is the simulated historic average Temperature of 28 years derived from each climate model for the month i . These variables have the exact definition for precipitation

(Massah and Morid, 2005; Mosadegh and Babaeian, 2022; Kalhori *et al.*, 2022).

Rainfall-Runoff Simulation and Drought Analysis

The IHACRES semi-conceptual model is suitable for predicting discharge used for climate change scenarios (Jakeman and Hornberger, 1993). In this study, climate indicators including Z score, SIAP, SPI, and BMDI (Li *et al.*, 2019) have been used to calculate the impacts of droughts in the current and future projections. Hydrological indicators determine the hydrological drought status based on one or more parameters, including river discharge, snow and rainfall, and reservoir storage volume. SWSI and SDI (Van Loon, 2015) drought indices were used annually to monitor hydrological drought.

Estimation of Water Use in CROPWAT

Warmer future climate change would increase evaporation and cause increase in water use in irrigated agriculture, urban demand, and water-dependent ecosystems (World Bank, 2016). ETC_t is crop water requirement in month t (mm month⁻¹) achieved according to Equation (6) and the KC_t is crop coefficient in month t and ETo_t is Reference crop Evapotranspiration.

$$ETC_t = ETo_t \times KC_t \quad (6)$$

The KC coefficients are extracted from FAO56. Cultivation pattern and cultivation percentage are considered based on the data given by AJO Dehloran (Table2).

Simulation and Optimization by SOP and Nash Bargaining Optimization (NBO)

Models in water resources engineering are divided into three categories: optimization, simulation, and simulation-optimization (Dagan and Volji, 1993). The WEAP model is a computational tool for integrated water resource planning based on water balance equations. It can be applied to urban and agricultural systems, catchments, or



complex water systems. This model uses a Standard Operation Policy (SOP) to solve water allocation problems at each time step (Zarezadeh, 2011). In the current methodology, the groundwater simulation by the WEAP model is assumed as a large reservoir. It can be coupled with the Modflow model to simulate the distributed groundwater supply in the study area to consider the spatial groundwater changes. The water resources and consumptions schematic of the Doiraj Sub-Basin is depicted in Figure 3.

The method of conflict resolution is based on the bargaining theory proposed by Nash in 1953. In this study, all data information obtained from Ilam AJO and Ilam RWC, the utility functions of each sector presented in Figure 4 and the objective function and constraints are introduced in Equations (7)-(13).

$$\text{Max. } U = \prod (U_x(f_x) - U_x(d_x))^{w_x} \quad \text{for } x = a, i, d \quad (7)$$

$$f_x = \sum_{t=1}^T \frac{R_{x,t}}{D_{x,t}} \quad \text{for } x = a, i, d \quad \text{and } t = 1, \dots, T \quad (8)$$

Subject to:

$$R_{x,t} \leq \quad (9)$$

$$D_{x,t} \quad \text{for } x =$$

$$a, i, d \quad \text{and } t = 1, \dots, T$$

$$R_t = R_{a1,t} + R_{a2,t} + R_{i,t} + R_{d,t} \quad (10)$$

$$S_{t+1} = S_t + I_t - R_t -$$

$$L_t \quad \text{for } t = 1, 2, \dots, T \quad (11)$$

$$S_{\min} \leq S_t \leq$$

$$S_{\max} \quad \text{for } t =$$

$$1, 2, \dots, T$$

$$S_1 = S_{T+1} \quad (13)$$

In the above equations, f_x , d_x , and w_x represent the total supply to demand, the point of disagreement, and the relative weight of sector x , respectively. X expressed as a, i, d for the agricultural, industrial, and environmental sectors. It is noted that the relative weight of each sector is determined

according to the allocation priorities. $R_{x,t}$ represents the water allocated to demand $D_{x,t}$ of sector x per month t . R_t is the total amount of water released from the reservoir, I_t the amount of reservoir Inflow, S_t the reservoir Storage, and L_t the amount of reservoir Losses per month t . T is equal to the total number of periods. S_{\min} , and S_{\max} are the maximum and minimum possible values of the Storage volume in the reservoir, respectively. Also $U_x(d_x)$ and $U_x(f_x)$ are the level of Utility of the point of disagreement and the point of the required percentage of sector x , respectively. MATLAB software was used as a platform

to optimize the three-objective function by the GA algorithm.

To consider the disaggregation method for the future projections, the changes in precipitation and temperature based on the weighted method and drought indices are used as inputs of the WEAP and NBO models to meet the water demands based on their priority and utility functions.

Performance Criteria

To evaluate the efficiency of water resource systems, time-based reliability, volumetric reliability and resilience coefficients (Zarghami and Szidarovszky, 2011) are used in Equations (14) to (16).

Table 2. Percentage of crops in the proposed cropping pattern of the area.

Crops	Wheat	barley	Alfalfa	corn	Canola	Sugar beet	tomato	Vegetables	watermelon	Cucumber
Percentage of crops	25%	25%	3%	20%	13%	3%	4%	3%	2%	5%

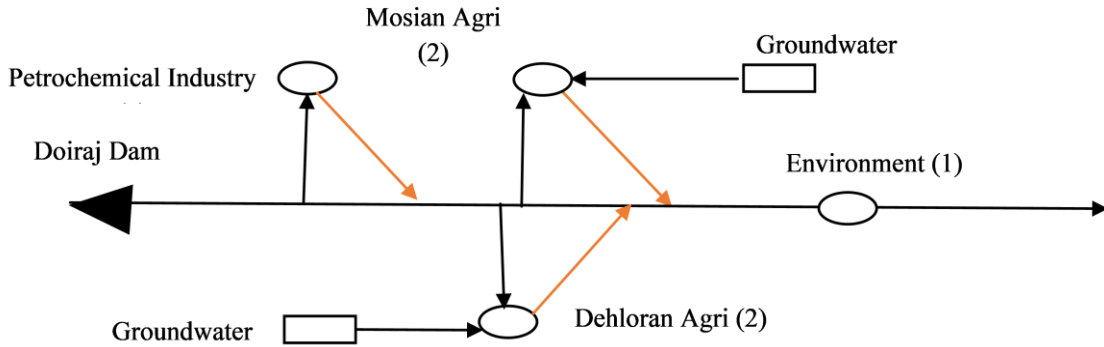


Figure 3. Water resources and consumptions schematic of the Doiraj sub-basin.

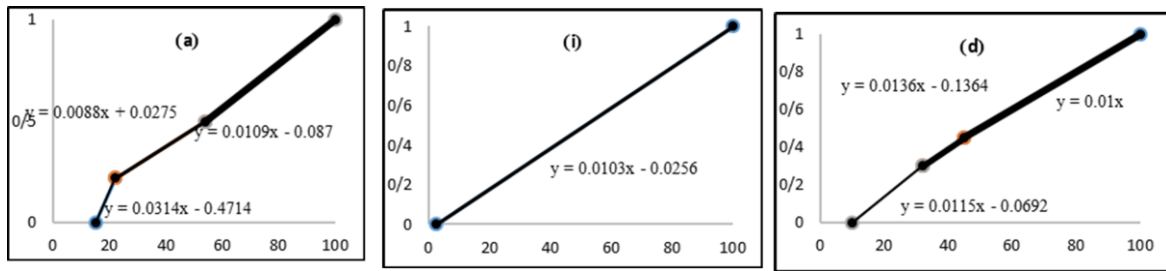


Figure 4. Utility functions of agricultural sectors (a), environment (i) and industry (d).

$$\alpha_{Tn-x}^T = \left(1 - \frac{\text{Number of failures during design period}}{\text{Length of design period (Monthly)}}\right) \times 100 \tag{14}$$

Where, α_{n-x}^T is the time-based reliability of supplying the requirement of sector x . The volumetric reliability of the reservoir system for the water allocation to x -th part (α_{n-x}^T) is obtained from the following relation:

$$\alpha_{v-x}^T = \frac{100}{T} \sum_{t=1}^T \left(\frac{R_{x,t}}{D_{x,t}}\right) \tag{15}$$

In this regard, T is the number of months in the planning horizon, $R_{x,t}$ and $D_{x,t}$ are, respectively, the amount of water allocated and requirement of x -th part. Resilience is a measure to determine if a system enters a failure state, how quickly it passes through it and enters the desired state (Ganji *et al.*, 2007).

$$\text{Res}^j = \frac{N(D_{t+1}^j = 0 : D_t^j > 0)}{N(D_t^j > 0)} \tag{16}$$

Where, D_t is Deficit in month t and N is the Number of situation that in the numerator shows number of satisfactory ($D_{t+1}^j = 0$) comes after unsatisfactory ($D_t^j > 0$). Where, D_t is Deficit in month t . N is the Number of situations.

RESULTS AND DISCUSSION

To study the effects of climate change on climatic variables and predict runoff and, consequently, drought monitoring of Doiraj

Table 3. Performance criteria of CMIP5 models compare to the observed precipitation and temperature.

model	Temperature				Rainfall			
	R ²	NSE	MAE	RMSE	R ²	NSE	MAE	RMSE
Weighted composition	0.98	0.97	0.94	1.03	0.98	0.97	1.40	6.46
Access1-0	0.98	0.97	1.37	1.43	0.92	0.86	4.53	13.65
Bcc-csm1-1	0.98	0.98	0.98	1.03	0.92	0.92	0.69	10.14
Bnu-esm	0.97	0.97	1.31	1.42	0.86	0.85	3.31	14.04
Canesm2	0.98	0.96	1.66	1.75	0.87	0.83	3.13	14.83
Csirok3-6-0	0.96	0.98	1.12	1.17	0.97	0.96	1.24	6.27
Fgoals-g2	0.98	0.97	1.33	1.46	0.95	0.92	4.06	10.22
Had-gem2-cc	0.97	0.96	1.57	1.63	0.98	0.74	11.33	18.47
Micro5	0.98	0.98	1.21	1.27	0.91	0.88	4.17	12.59
Fio-esm	0.98	0.98	1.01	1.09	0.89	0.82	3.83	15.37
Mri-cgm3	0.98	0.98	1.30	1.34	0.93	0.88	4.81	12.60

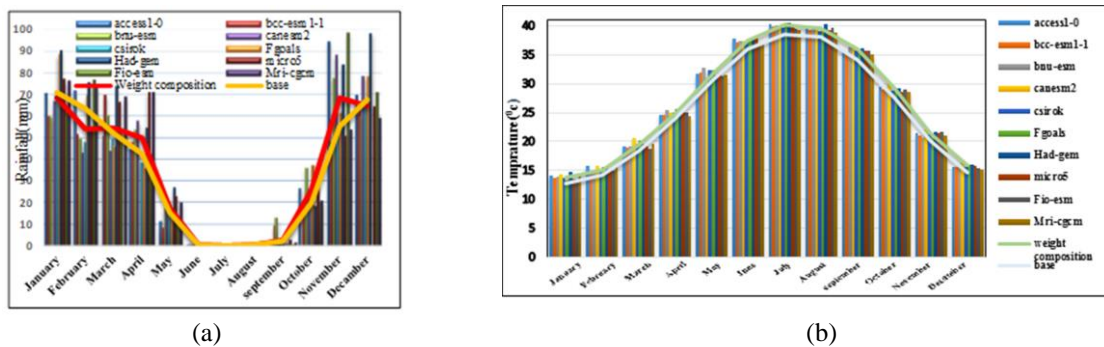


Figure 5. Simulated and observed rainfall (a) and temperature (b) under RCP8.5 scenario.

Dam in Dehloran City, the outputs of 10 CMIP5 models under the RCP8.5 were used.

Rainfall and Temperature Changes in Climate Models

MOTP method was used to interfere with the uncertainty of the models, which determined the weight of the precipitation and the temperature of the models based on their similarity to the observed data. To evaluate the performance of the models, the R², NSE, RMSE; and MAE were calculated and presented in Table 3.

The combined model to simulate the precipitation and temperature was more reliable due to uncertainty analysis. Figure 5 shows the precipitation and temperature of each climate model.

The results of the weighted composition model showed that precipitation increased by 4.39% and temperature by 5.04°C compared to the baseline period. Also, in winter, the slightest difference between the long-term average rainfall of baseline and future was observed in the Had-gem model in January, while the highest was in the Csirok3-6 in March. In spring, the lowest difference was observed in June using the weighted composition model, while the highest was in April by the Mri-cgcm. In summer, the lowest difference was in July by the Bnu-esm, while the highest difference was indicated in September using the Bnu-esm. In the fall, the lowest and highest differences between baseline and future

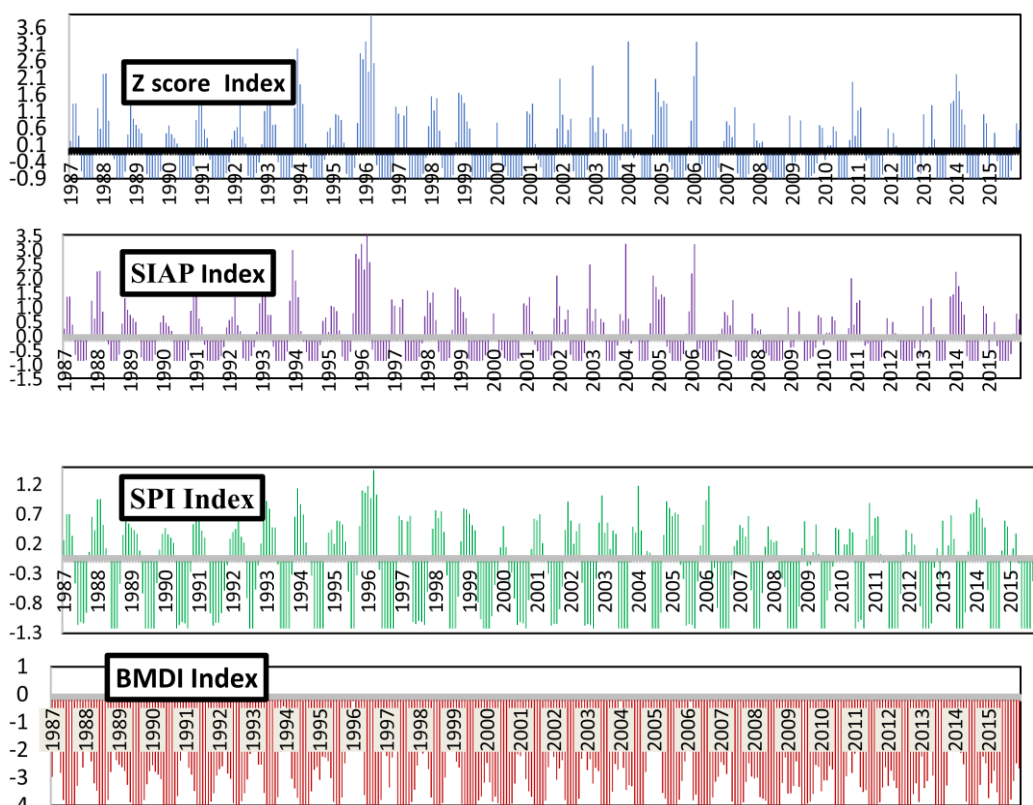


Figure 6. Drought Indicators in the Doiraj Dam Station during 1987-2015.

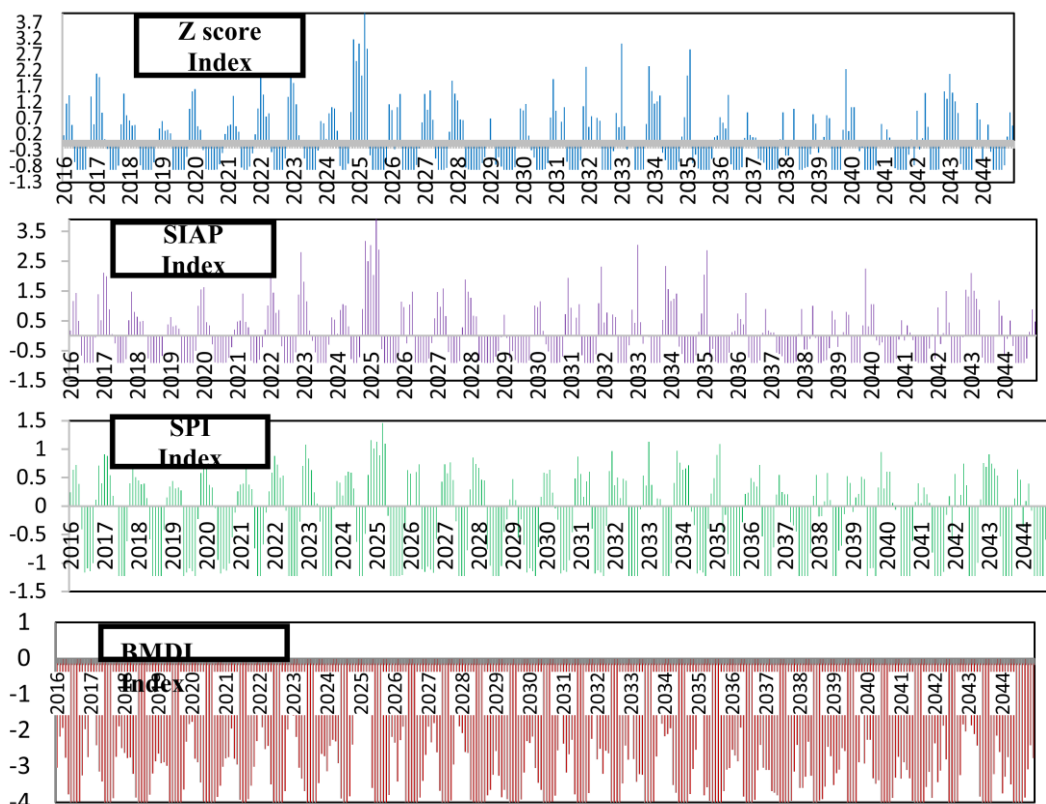


Figure 7. Drought Indicators in the Doiraj Dam Station during 2016-2044.



rainfall events were obtained, respectively, in October and November by Fio-esm. All models showed a relative increase in temperature.

Meanwhile, the highest difference was observed in May using the Bnu-esm, while the lowest difference was in April by the Mri-cgcm during the spring season. In summer, the lowest and highest differences were, respectively, in August using the Mri-cgcm and September by the Canesm2. The lowest difference in baseline and the future temperature was observed in December using the Mri-cgcm, and the highest in October by the Canesm2. A comparison between precipitation and temperature parameters in the observed and weighted composition model shows that the rainfall would increase in most months of the year during the future period. Still, there was a significant increase in precipitation in November and decline in February compared to the observation period. The temperature parameter shows an increase in all months, while the highest temperature rise occurs in July.

Drought Monitoring with Climate Indicators

Each climate index has a different range of changes: the more negative the indicators, the more severe drought conditions, and the more positive numbers, indicating fewer drought conditions and more humidity. The Doiraj Watershed drought for the current and future periods due to climate change is shown in Figures 6 and 7.

The Z score is predicted by 86 months of near-drought, 78 months relatively wet, 157 months relatively dry, and 27 months very wet in the observation period. Also, according to the SIAP index, the number of normal, very wet, wet, and dry months were 85, 54, 49, and 160, respectively. In the SPI chart, the number of relatively normal months is 227. They are 112 and 9 for dry and wet months. In the BMDI index, there are 143, 90, 31,75 and 9 months in relatively

dry, poor drought, very high drought, and normal conditions, respectively.

In the future period, the Z score is predicted by 87, 79, 157, and 25 months near normal conditions, relatively wet, relatively dry, and very wet, respectively. Also, according to the SIAP index, the number of normal, very wet, wet, and dry months were 85, 58, 160, and 45 months, respectively. The SPI index has shown 229, 109, and 10 relatively normal conditions, relatively dry, and relatively humid, respectively. Also, BMDI index showed 148, 87, 70, and 13 dry, relatively dry, severely dry, and normal, respectively.

The comparison of this study with others (Norozi *et al.*, 2018; Guoyong *et al.*, 2015) shows that the meteorological drought will occur in the most severe cases in 2041, 2037, 2029, and 2028 for the Ilam Station.

Run off Simulation with IHACRES

The basin runoff was predicted by the IHACRES model for the ten CMIP5 and the combined model. The different years were tested to calibrate the model, and the results showed that the period (1987-2001) had the best performance criterion. The IHACRES calibration parameters are shown in Table 4. Model validation was selected for years 2002 to 2015.

The comparison results of the simulated and observed runoff hydrograph shows that the peak values have a proper compliance that are shown in Figure 8-a. The model validation for the time period 2002–2015 is in Figure 8-b.

The NSE is recommended as the best criterion for reflecting the overall fit of a hydrograph by Nash and Sutcliffe (1970), ASCE (1993), and Legates and McCabe (1999). The R^2 and NSE values greater than 0.6 and 0.5 could be recognized as the satisfactory model (Binaman and Shoemaker, 2005; Legates and McCabe, 1999; Nash and Sutcliffe, 1970). The predicted runoff from 2016 to 2044 for each model is shown in Figure 9.

Table 4. Calibrated parameters of IHACRES model.

Parameter	P	I	F	$\tau(w)$	C	
Explanations	Soil intensity	moisture	Moisture threshold	Coefficient of basin heating	of Dry ng time	Humidity storage capacity
Optimum amount	1.0	0.2	0.05	65.0	0.31	
Parameter	a(s)	$v^{(s)}$	$\tau(s)$	B(s)		
Explanations	Fatigue coefficient	Volume ratio	Slow down flow	Peak Index		
Optimum amount	-0.272	1.0	0.768	0.728		

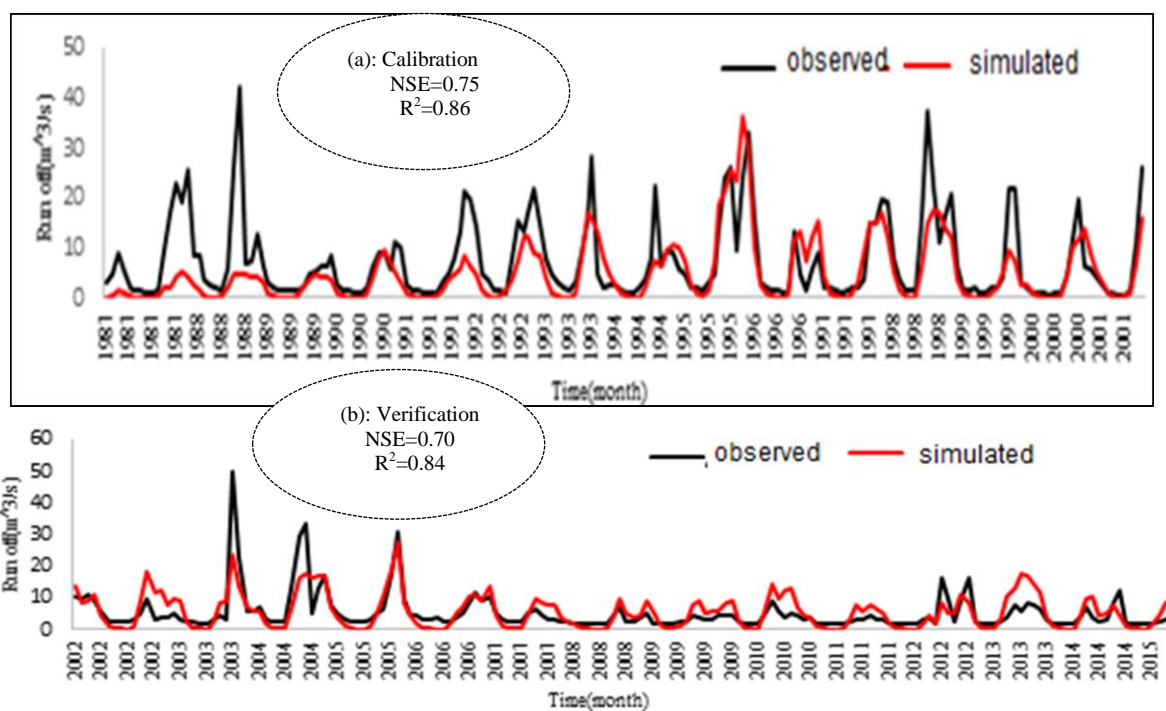


Figure 8- Simulation and observed runoff during the calibration period (a) and verification period (b) with IHACRES.

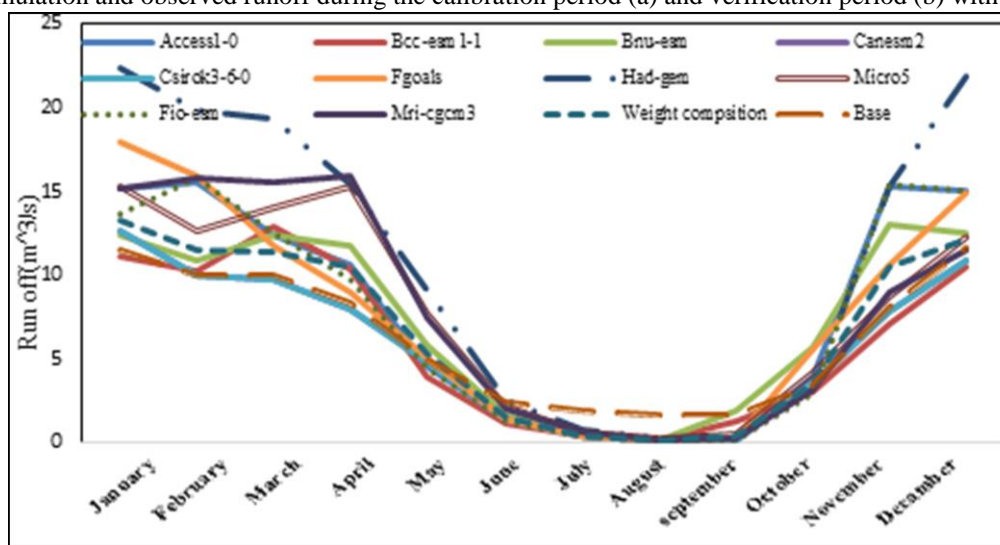


Figure 9. Comparison of the long-term monthly average of discharge.



The results show that in the next period, only two models predicted the runoff below the long-term average, while it increased for the other models. The combined model predicted the average reservoir inflow of $6.69 \text{ m}^3 \text{ s}^{-1}$, indicating an increase of 6.3% compared to the average observed runoff of reservoir inflow of $6.27 \text{ m}^3 \text{ s}^{-1}$.

Monitoring River Runoff with Hydrological Indicators

In this study, the hydrological drought indices are performed by the SWSI and SDI in the current and future projections, as shown in Figure 10.

Surveys of hydrological drought with SWSI index showed that a very dry classification with 20% has been added in the future projection rather than the current projection. It is a good match with the results of Norozi et al. (2018). The SDI index results showed no significant changes in the drought classification between the current and the future cases.

Water Demand Simulation in CROPWAT

The CROPWAT model was used to calculate the actual amount of crop water requirement for the current and future scenarios (Table 5). Water demand increased 104 % in future duration, which is critical to managing water allocation.

Current and Future Status of Water Resources Analysis in WEAP

The water allocation of the Doiraj Basin is simulated by the WEAP model under the current conditions with a cultivated area of 4880 hectares and an annual water requirement of 64.14 MCM supplied by a combination of surface and groundwater. Table 6 shows the results of supply to demand in the current and future situation.

According to Table 6, the annual average water supply of the agricultural sector increased from the current 95.3 to 96.3% in the future projection, unlike the industrial

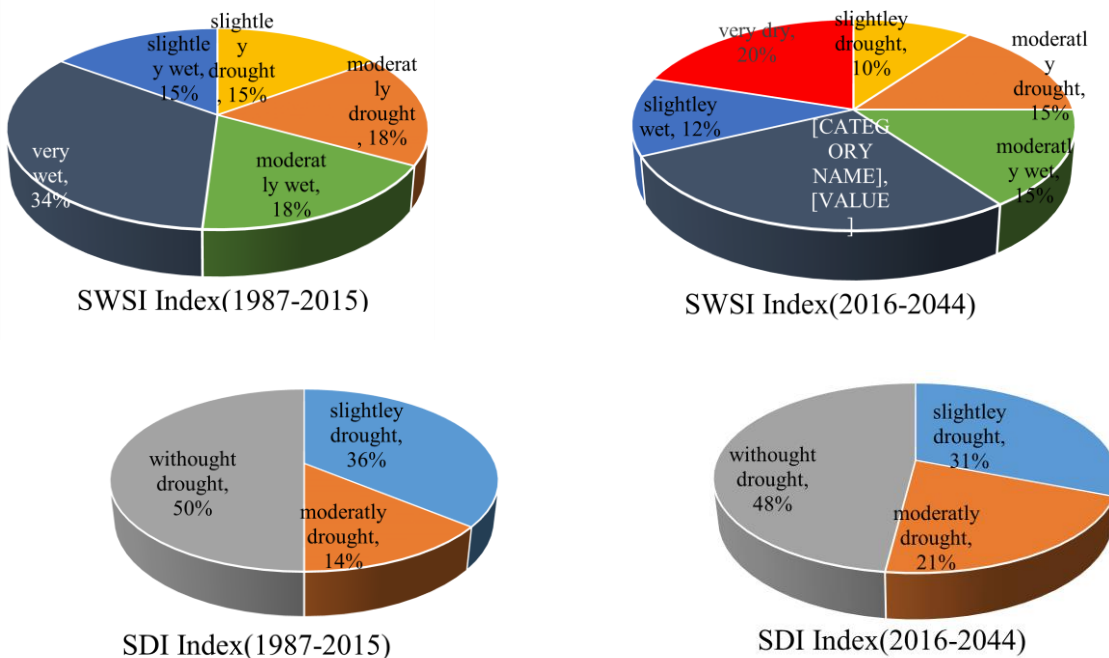


Figure 10. Status of SWSI and SDI index in the period of 1987-2015 and 2016-2044.

and environmental demands, which which have decreased by about 7-8%. This happened due to the supplying agricultural demand by 12.5 MCM of groundwater and 104.75 (MCM) of river flow and reservoir release.

The results of the water resources and consumption simulation in this study show that the WEAP model was able to provide acceptable results based on the supply priorities, which is consistent with the studies of Mehrparvar *et al.* (2019). For optimal allocation based on the utility functions of each stakeholder, the NBO method is used, which is also mentioned in studies of Sharifazari *et al.* (2021).

Water Allocation Optimization based on NBO

To derive optimal operation rules, the effective model parameters were calibrated using sensitivity analysis by the NBO and GA, such as population size, elitism rate,

and stopping point. The convergence process and reaching the optimal solution were used for sensitivity analysis of the algorithm and determination of these parameters was estimated by trial and error. The detailed results are presented for the considered scenario in Table 7.

Table 7 shows the obtained optimal parameters for which the best performance is selected according to the convergence process of the objective function. Second run with a population size of 2088, a crossover fraction of 0.75 and a stopping criterion of 18000 seconds is selected from other runs.

For the sensitivity analysis, the priority levels and relative weights for different sectors are considered and presented in Table 8.

Based on the current studies, the GA model can assign the allocations related to each stakeholder in less time and more accurately based on the utility functions and the Nash objective function, which is also mentioned in the studies of Jeong and Kang

Table 5. Water demand for the agricultural sector in terms of current and future scenario (MCM).

Month	Jan	Feb	Mar	Apr	May	June	July	Aug	Sep	Oct	Nov	Dec	sum
current situation	0	0.634	20.398	11.102	24.571	5.758	0	0	0	0.317	1.366	0	64.148
Future scenario	0	0	22.748	32.948	61.517	10.359	0	0	0	0	3.311	0	130.883

Table 6. The percent of supply to demand by the WEAP Model (%).

Month		Jan	Feb	Mar	Apr	May	June	July	Aug	Sep	Oct	Nov	Dec	Ann
Agriculture	Current	100	100	92.9	85.0	83.9	82.1	100	100	100	100	100	100	95.3
	Future	100	100	99.8	97.1	83.6	75.9	100	100	100	100	99.7	100	96.3
Industry	Current	96.5	100	86.0	82.5	77.5	75.0	85.0	95.0	84.0	86.0	100	100	89.0
	Future	100	100	100	89.5	69.0	64.5	58.5	55.0	55.5	85.0	100	100	81.4
Environment	Current	100	100	100	89.6	85.3	97.2	100	100	97.2	97.8	100	100	97.3
	Future	100	100	100	100	88.9	70.1	74.2	94.0	83.1	78.1	100	100	90.7

**Table 7.** Sensitivity analysis of effective parameters in achieving the optimal solution in GA.

Optimal model	Effective parameter	Run1	Run2	Run3	Run4	Run5	Run6
GA	Stopping point (Time-seconds)	18000	18000	2160 0	25200	2880 0	32400
	Crossover fraction	0.5	0.75	0.75	0.5	0.75	0.75
	The population size	2088	2088	2088	2088	2088	2088

Table 8: Relative weight of sensitivity analysis in GA algorithm.

Stakeholders	Priority	Run1	Run2	Run3	Run4	Run5
Agriculture	3	0.3	0.35	0.25	0.3	0.15
environmental	1	0.5	0.5	0.6	0.6	0.7
Industry	2	0.2	0.15	0.15	0.1	0.15

(2021) and Sharifazari *et al.* (2021).

Comparing Reservoir Operation Policy in GA and WEAP

The water allocated to each sector by the WEAP and GA models in the future scenarios 2016 to 2044 under drought conditions is in Figure 11.

Comparing the performance of the WEAP and GA models on the water supply of different demands shows that the GA model is more reliable than the WEAP model. Although there is no month with 100% satisfaction in the GA model, the minimum satisfaction is 80% for all demand sectors. However, in the WEAP model, there are some months with 100% and less than 50% satisfaction. In other words, the smart operation policy is established by the NBO algorithm in the GA model like hedging operation policy. The reservoir storage volume variations for both models are shown in Figure 12.

It indicates that 50% of the time, the reservoir storage volume is more than 37 MCM. The reservoir storage volume in the SOP method in 44% of the cases is higher than in the NBO method. Also in this method, Reservoir storage duration curve shows that, the reservoir is completely full in 10% of the time and it's completely empty in 20% of the

time.. On the other hand, in the NBO method, the minimum reservoir storage is about 18 MCM, and it is never full or empty. Therefore, this operation policy can prevent severe deficit and reservoir losses through the spill and evaporation.

By comparing the results of this study with Homayounfar *et al.* (2015) and Jeong and Kang (2021), the Nash model can optimize water allocation and provide a suitable operation policy to resolve the conflict between the stakeholders and their utility functions. Considering the studies of Sharifazari *et al.* (2021), the convergence speeds of the GA are slightly faster than the ACOR. Meanwhile, based on the NBO model, the GA method performed better than ACOR in all three scenarios for objective function. Therefore, to meet the objective function, this method is recommended for conflict resolution in the basins.

Reservoir's Performance Criteria

Investigation of the performance criteria of the optimal model compared to the simulation model shows that the time reliability of agricultural, environmental, and industrial sectors in the GA model is better than the WEAP model. Table 9 shows the performance criteria of the two models.

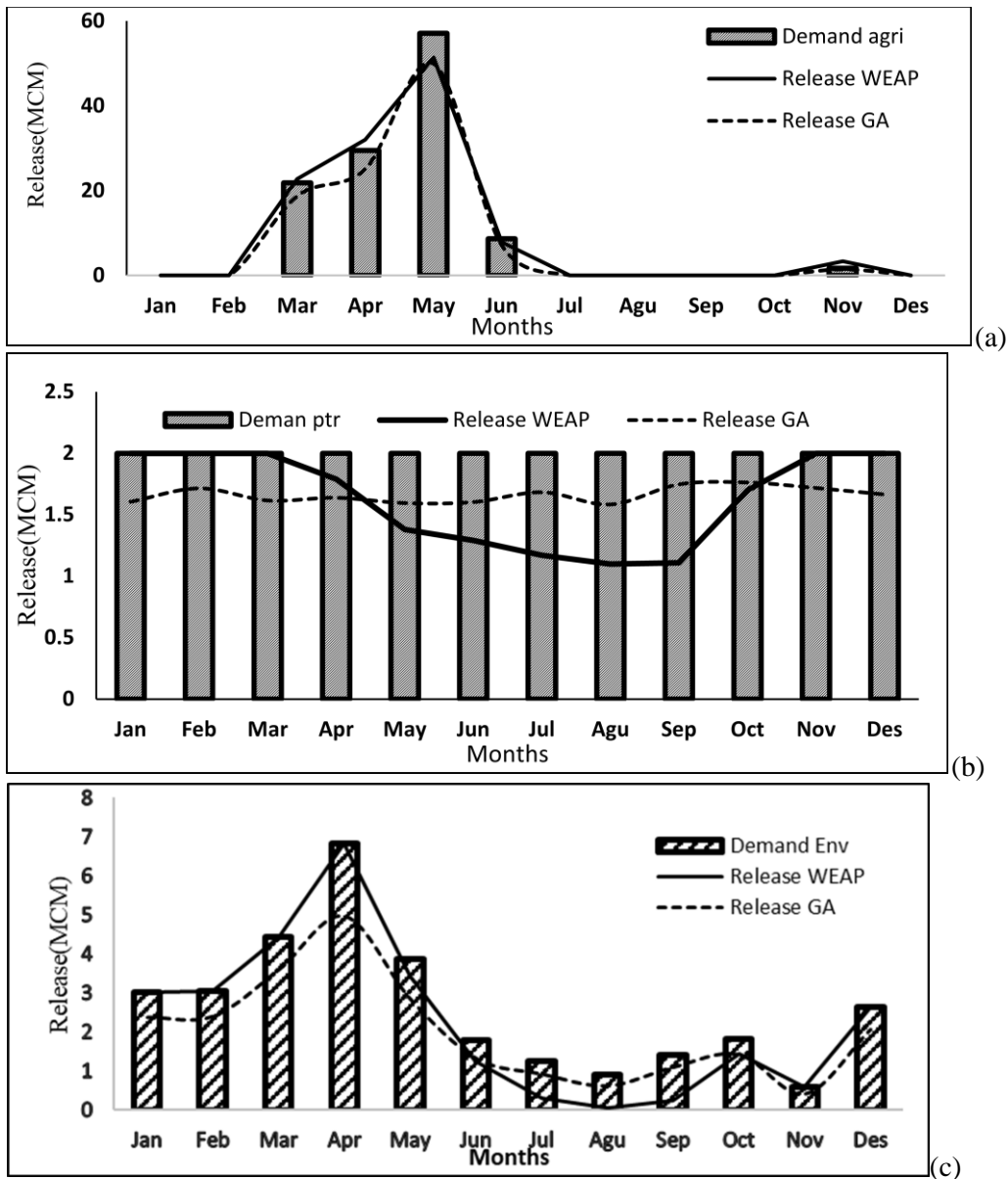


Figure 11. Demand and supply for agricultural (a), industrial (b), and environmental (c) stakeholders during the (2016-2044).

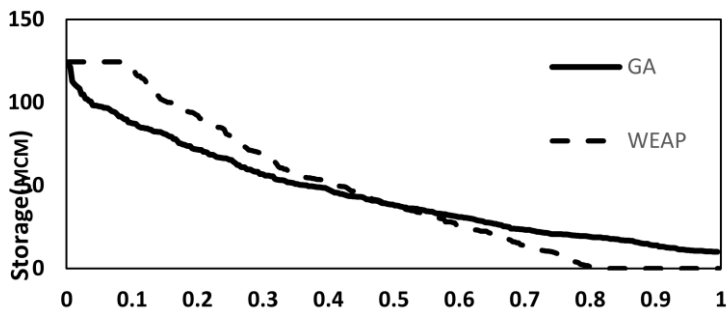


Figure 12. Reservoir storage duration curve (2016-2044).



The highest time reliability coefficient among the three stakeholders belongs to the environmental sector, while the least is for the industry. In the GA model, for agricultural requirement as the largest stakeholder, the coefficients of volumetric reliability, resilience, and time-based reliability are 0.90, 0.76, and 0.9, respectively.

CONCLUSIONS

In this study, in Doiraj Watershed, the effects of climate change on runoff prediction and two different water policies for allocating water to stockholders are considered by the WEAP and NBO models. The assessment of 10 CMIP5 GCM models showed that the changes in precipitation and temperature are generally estimated as +4.35% and 5.04°C. The future runoff uncertainty is mainly due to the precipitation that comes through GCMs.

The future runoff simulation is modeled by the IHACRES, and the future runoff results indicate that it would be increased by 6.3% during the future period in comparison to the current status. In this way, the simulated water demand would increase 104% by the CROPWAT model due to the increase in temperature and agricultural land use in the future.

In this basin, there are significant conflicts between Regional Water Organization and Agricultural Jihad Organization to supply the industrial water demands and more agricultural development. The optimal amount of agricultural, industrial, and environmental uses are determined by the game theory and the NBO in the current and future conditions. In this regard, the desirability of each stakeholder is properly provided. The volumetric reliability, resilience, and time-based reliability coefficients for agricultural water demand, as the largest stakeholder in the GA model, were found as 0.90, 0.76, and 0.9, respectively.

The analysis of the reservoir storage duration curve shows that the SOP policy in the WEAP model causes the reservoir storage to be completely full in 10% of the time and completely empty in 20% of the time, while in the NBO method, the reservoir is never completely full or empty and can manage reservoir storage in drought conditions.

List of acronyms

ACOR: Ant Colony Optimization Release
AJO: Agricultural Jihad Organization
AR5: Fifth Assessment Report
CMIP5: Coupled Model Inter comparison Project 5
DIC: Drought Indices Calculator
GA: Genetic Algorithm
GCM: General Circulation Model
GMCR: Graph Model for Conflict Resolution and Decision Support
Ha: Hectares

IHACRES: Identification of unit Hydrograph and Component flows from Rainfall, Evapotranspiration and Stream flow
IPCC: Intergovernmental Panel on Climate Change
IRWC: Isfahan Regional Water Company
KRWC: Kermanshah Regional Water Company
KPMA: Kermanshah Province Meteorological Administration
MAE: Mean Absolute Error
MCM: Million Cubic Meter
MOTP: Mean Observed Temperature – Precipitation
NBO: Nash Bargaining Optimization
NSE: Nash–Sutcliffe efficiency
R²: determination Coefficient
RCP: Representative Concentration Pathway
RMSE: Root Mean Square Error
RWO: Regional Water Organization
SOP: Standard Operation Policy
TAR: Third Assessment Report
WEAP: Water Evaluation and Planning.

ACKNOWLEDGEMENTS

The authors would like to thank KRWC and KPMA. The authors received no financial support for the research, authorship, and publication of this article.

REFERENCES

- ASCE. 1993. Criteria for Evaluation of Watershed Models. *J. Irrig. Drain. Eng.*, **119(3)**: 429-442.
- Azadi, F., Ashofteh, P. S. and Loáiciga, H. A. 2019. Reservoir Water-Quality Projections under Climate-Change Conditions. *Water Resour. Manage.*, **33**: 401-421.
- Binaman, J. and Shoemaker, C.A. 2005. An Analysis of High-Flow Sediment Event Data for Evaluating Model Performance. *Hydrol. Process.*, **19**: 605-620.
- Bozorg-Haddad, O., Athari, E., Fallah-Mehdipour, E. and Loáiciga, H. 2018. Real-Time Water Allocation Policies Calculated with Bankruptcy Games and Genetic Programming. *Water Supply*, **18(2)**: 430-449.
- Christensen, J. H., Kjellström, E., Giorgi, F., Lenderink, G., Rummukainen, M., 2010, Weight Assignment in Regional Climate Models. *Climate Res.*, **44**: 179-194.
- Coppola, E. 2000. Optimal Pumping Policy for a Public Supply Well Field Using Computational Neural Network with Decision-Making Methodology. Doctoral Dissertation, Univ. Arizona, 226 PP.
- Dagan, N. and Volji, O. 1993. The Bankruptcy Problem: A Cooperative Bargaining Approach. *Math. Soc. Sci.*, **26(3)**:287-297.
- Frisvold, G. B. and Caswell, M. F. 2000. Trans Boundary Water Management Game-Theoretic Lessons for Projects on the US-Mexico Border. *Agric. Econ.*, **24(1)**: 101-111.
- Fu, J., Zhong, P., Zhu, F., Chen, J., Wu, Y. and Xu, B. 2018. Water Resources Allocation in Trans Boundary River Based on Asymmetric Nash-Harsanyi Leader-Follower Game Model. *Water*, **10(3)**: 270.
- Ganji, A., Karamouz, M. and Khalili, D. 2007. Development of Stochastic Dynamic Nash Game Model for Reservoir Operation II. The Value of Players' Information Availability and Cooperative Behaviors. *Adv. Water Resour.*, **30(1)**: 157-168.
- Giorgi, F. and Francisco, R. 2001. Uncertainties in the Prediction of Regional Climate Change. In: "*Global Change and Protected Areas*", (Eds.): Visconti, G., Beniston, M., Iannorelli, E. D. and Barba, D. *Advances in Global Change Research 9*, Springer, Dordrecht.
- Guoyong, L., Qihong, T. and Scott, R. 2015. Climate Change Impacts on Meteorological, Agricultural and Hydrological Drought in China. *Glob. Planet. Change*, **126**: 23-34 .
- Homayounfar, M., Zomorodian, M., Martinez, Ch. and Lai, S. H. 2015. Two Monthly Continuous Dynamic Model Based on Nash Bargaining Theory for Conflict Resolution in Reservoir System. *PloS One*, **10(12)**: e0143198.
- IPCC. 2013. Summary for Policymakers. In: "*Climate Change: The Physical Science Basis*", (Eds.): Stocker, T. F., Qin, D., Plattner, G. K., Tignor, M., Allen, S. K., Boschung, J., Nauels, A., Xia, Y., Bex, V. and Midgley, P. M. Contribution of Working Group I to the Fifth Assessment Report of the Intergovernmental Panel on Climate Change, Cambridge University Press, Cambridge, United Kingdom and New York, NY, USA.
- Jakeman, A.J. and Hornberger, G. M. 1993. How Much Complexity Is Warranted in a Rainfall-Runoff Model, *Water Resour. Res.*, **29**: 2637-2649.
- Jeong, G. and Kang, D. 2021. Hydro-Economic Water Allocation Model for Water Supply Risk Analysis: A Case Study of Namhan River Basin, South Korea. *Sustainability*, **13(11)**: 6005.
- Jones, R. N. 2000. Managing Uncertainty in Climate Change Projections- Issues for Impact Assessment. *Clim. Change*, **45**: 403-419
- Kaini, S., Nepal, S., Pradhananga, S., Gardner, T. and Sharma, A. 2020. Impacts of Climate Change on the Flow of the Transboundary Koshi River, with Implications for Local Irrigation. *Int. J. Water Resour. Dev.*, **37(6)**: 929-954.
- Kalhor, M., Ashofteh, P. S. and Moghadam, S. H. 2022. Investigating the



- Effect of Uncertainty of AOGCM-TAR and AOGCM-AR5 Climate Change Models on River Runoff. *Arab. J. Geosci.*, **15**: 1198.
20. Kuriqi, A., Pinheiro, A. N., Sordo-Ward, A. and Garrote, L. 2019. Influence of Hydrologically Based Environmental Flow Methods on Flow Alteration and Energy Production in a Run-of-River Hydropower Plant. *J. Clean. Prod.*, **232**: 1028-1042.
 21. Lambert, S. J. and Boer, G. J. 2001. CMIP1 Evaluation and Intercomparison of Coupled Climate Models. *Clim. Dyn.*, **17(2-3)**: 83–106.
 22. Legates, D. R. and McCabe, G. J. 1999. Evaluating the Use of “Goodness-of-Fit” Measures in Hydrologic and Hydro Climatic Model Validation. *Water Resour. Res.*, **35(1)**: 233-241.
 23. Leong, W. K. and Lain, S. H. 2017. Application of Water Evaluation and Planning Model for Integrated Water Resources Management: Case Study of Langat River Basin, Malaysia. *IOP Conf. Ser.: Mater. Sci. Eng.*, **210** 012024.
 24. Li, F., Li, H., Lu, W., Zhang, G. and Kim, J. C. 2019. Meteorological Drought Monitoring in Northeastern China Using Multiple Indices. *Water*, **11(1)**:71
 25. Malka, L., Daci, A., Kuriqi, A., Bartocci, P. and Rrapaj, E. 2022. Energy Storage Benefits Assessment Using Multiple-Choice Criteria: The Case of Drini River Cascade. Albania. *Energies*, **15**: 4032.
 26. Massah Bavani, A. and Morid, S. 2005. Impacts of climate change on water resources and food production: a case study of Zayandeh-Rud-Basin, Esfahan, Iran. *J. Water Resour. Res.*, **1**: 40- 47. (in Persian with English abstract).
 27. Mehrparvar, M., Ahmadi, A. and Safavi, H. R. 2019. Resolving Water Allocation Conflicts Using WEAP Simulation Model and Non-Cooperative Game Theory. *Simulation*, **96(1)**: 17-30.
 28. Moghadam, S. H., Ashofteh, P. S. and Loáiciga, H. A. 2022. Optimal Water Allocation of Surface and Ground Water Resources under Climate Change with WEAP and IWOA Modeling. *Water Resour. Manag.*, **36**: 3181–3205.
 29. Mosadegh, E. and Babaeian, I., 2021. Projection of Temperature And Precipitation For 2020-2100 for Tehran Region Using Post-processing of General Circulation Models Output And Artificial Neural Network Approach. arXiv:2109.04619 [physics.aoph]
 30. Naghdi, S., Bozorg-Haddad, O., Khorsandi, M. and Chu, X. 2021. Multi-Objective Optimization for Allocation of Surface Water and Groundwater Resources. *Sci. Total Environ.*, **776**: 146026.
 31. Nash, J. E. and Sutcliffe, J. V. 1970. River Flow Forecasting through Conceptual Models Part I: A Discussion of Principles. *J. Hydrol.*, **10**: 282–290.
 32. Norozi, E., Rostami, N. and Jahangir, M. 2018. Prediction of Drought Condition during 2018-2037 Period under Climate Change Approach (Case Study: Ilam and Dehloran Stations). *Iran. J. Ecohydrol.*, **5(3)**: 977-991. (in Persian with English Abstract)
 33. Ransmeier, J. S. 1942. The Tennessee Valley Authority: A Case Study in the Economics of Multiple Purpose Stream Planning. Vanderbilt University Press, Nashville (Tennessee).
 34. Ratner, B., Burnley, C., Mugisha, S., Madzudzo, E., Oeur, I., Mam, K., Rüttinger, L., Chilufya, L. and Adriázola, P. 2018. Investing in Multi-Stakeholder Dialogue to Address Natural Resource Competition and Conflict. *Dev. Pract.*, **28**: 799-812
 35. Serrano, R. 2021. Sixty-Seven Years of the Nash Program: Time for Retirement. *SERIEs*, **12**: 35–48.
 36. Sharifazari, S., Sadat-Noori, M., Rahimi, H., Khojasteh, D. and Glamore, W. 2021. Optimal Reservoir Operation Using Nash Bargaining Solution and Evolutionary Algorithms. *Water Sci. Eng.*, **14(4)**: 260-268.
 37. Van Loon, A. F. 2015. Hydrological Drought Explained. *WIREs Water*, **2(4)**: 359-392.
 38. Wilby, R. L. and Harris, I. 2006. A Framework for Assessing Uncertainties in Climate Change Impacts: Low-Flow Scenarios for the River Thames, UK. *Water Resour. Res.*, **42(2)**: 1-10.
 39. World Bank. 2016. *High and Dry: Climate Change, Water, and the Economy*. License: Creative Commons Attribution CC BY 3.0 IGO, Washington, DC.
 40. Zarezadeh, M. 2011. Water Allocation in the Qezelozan-Sefidrood Basin under Climate Change, 20 using Bankruptcy

- Approach for Conflict Resolution, MS. Thesis, Dep. of Water Resources Engineering, Tarbiat Modares University, Tehran, Iran.
41. Zarghami, M. and Szidarovszky, F. 2011. Multi Criteria Analysis Applications to Water and Environment Management. Textbook, Springer, PP. 95-104.
42. Zheng, H., Chiew, F. H. S., Charles, S. and Podger, G. 2018. Future Climate and Runoff Projections across South Asia from CMIP5 Global Climate Models and Hydrological Modelling. *J. Hydrol.: Reg. Stud.*, **18**: 92-109.

بهینه سازی چانه زنی نش برای آب رها شده از سد مخزنی در شرایط تغییر اقلیم (مطالعه موردی: سد دویرج)

ز. پورخیراله، م. حافظ پرست مودت، و س. ا. فاطمی

چکیده

تقاضای فزاینده ای برای حل تعارضات بین مصرف کنندگان و ذینفعان مختلف آب تحت شرایط تغییر اقلیم وجود دارد. در این مطالعه ده مدل اقلیمی CMIP5 تحت سناریوی RCP8.5 برای شبیه سازی تخصیص آب مخزن سد دویرج در استان ایلام استفاده شده است. برای کاهش عدم قطعیت مدل های اقلیمی، از روش MOTP با ترکیب مدل های مختلف GCM استفاده شد. به منظور پیش بینی جریان ورودی مخزن، مدل بارش-رواناب آبهکرس برای دوره های زمانی ۲۰۱۶ تا ۲۰۴۴ در نظر گرفته و اعتبارسنجی شد. شاخص های اقلیمی و هیدرولوژیکی برای پایش دوره های خشکسالی در پیش بینی های فعلی و آینده استخراج شده است. مدل WEAP و روش چانه زنی نامتقارن نش به ترتیب برای شبیه سازی سیستم حوضه آب و حل تعارض بین ذینفعان مختلف بر اساس توابع مطلوبیت آنها استفاده شد. نتایج حاکی از آن است که میزان بارندگی در دوره آبی در فصل بهار و پاییز به ترتیب ۱/۱۷ و ۱/۱۱ درصد افزایش و در زمستان ۹/۴ درصد کاهش می یابد. همچنین بالاترین نرخ رشد دما و رواناب در شهریور ۱/۹۵ درجه سانتی گراد و ۶/۳ درصد در مقایسه با دوره پایه افزایش یافته است در حالی که تقاضا به میزان ۵۵/۷۵ درصد افزایش می یابد. کمبود بلندمدت کشاورزی با مدل WEAP در شرایط فعلی و آینده به ترتیب ۱۰.۹٪، ۱۰.۲٪ به دست می آید. در نهایت، منحنی تداوم حجم مخزن نشان داد که ۲۰ درصد از مواقع ذخیره سازی مخزن برای روش بهره برداری SOP خالی است. با تغییر به سیاست چانه زنی نش، نه تنها حداقل ظرفیت ذخیره سازی برای همیشه به ۱۸ م.م می رسد، بلکه اثرات تغییرات آب و هوایی نیز در آینده تطبیق داده می شود و توابع مطلوبیت ذینفعان نیز برآورده می شوند.